Imperial College London

MSc Applied Mathematics Project

Imperial College London

Department of Mathematics

Advanced Numerical Algorithms for the Simulation of Weather Fronts

Author:
Chloe Raymont

CID:
00733439

Supervisor:
Dr. Colin Cotter

Second Marker:

September 6, 2018

Abstract

Your abstract goes here

Acknowledgements

Declaration

The work contained in this thesis is my own work unless otherwise stated

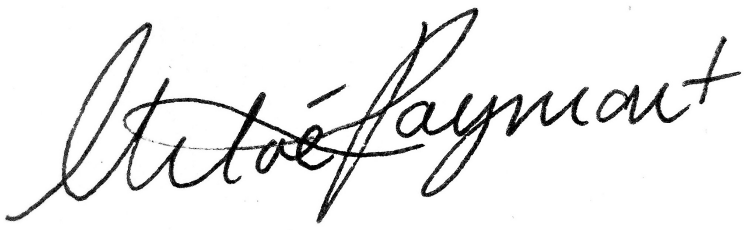

Contents

List of Figures

Chapter 1

Introduction

Chapter 2

The Governing Equations

The semi-geostrophic equations first introduced by [1] form the basis of our model for frontogenesis. Widely noted to be more rigorous than the classical quasi-geostrophic equations in their description of the formation of weather fronts [2, 3]. In this chapter a summary of key steps that lead to the Eady model for frontogensis that was developed by Hoskins and Bretherton , 1972, [4] is given. Based on the model for baroclinic instability proposed by Eady, 1949, incorporating a linear stratification in density and a constant vertical shear in the horizontal velocity component. A co-ordinate transform to geostrophic co-ordinates by [3] facilitates the numerical implementation of these equations and subsequent interpretation of results. For the following the main points are summarised from Cullen 2006 [2] in formulating the model to be implemented numerically.

2.1 The Semi-Geostrophic Equations

2.1.1 The 3D Incompressible Boussinesq Equations

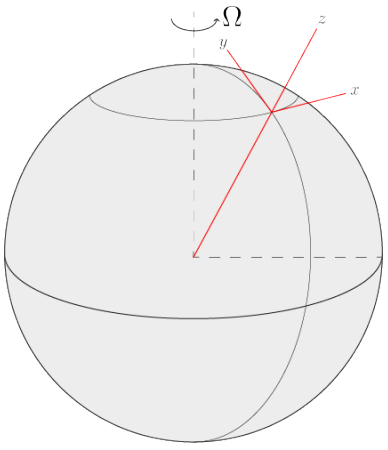

Figure 2.1: Local cartesian co-ordinates (x, y, z) on Earth

We begin with the 3D incompressible Boussinesq equations 2.1 to describe atmospheric flow. Adopting cartesian co-ordinates (x, y, z) representing the zonal, meridional and radial directions on the Earth respectively, as shown in 2.1. The corresponding velocity components are $\boldsymbol{u} = (u, v, w)$, with ρ_0 representing the constant density and p denoting the pressure.

$$\begin{aligned} \frac{\mathrm{D}u}{\mathrm{D}t} - fv &= -\frac{1}{\rho_0}\frac{\partial p}{\partial x} \\ \frac{\mathrm{D}v}{\mathrm{D}t} + fu &= -\frac{1}{\rho_0}\frac{\partial p}{\partial y} \\ \frac{\mathrm{D}w}{\mathrm{D}t} &= -\frac{1}{\rho_0}\frac{\partial p}{\partial z} + b \\ \frac{\mathrm{D}b}{\mathrm{D}t} &= 0 \\ \nabla \cdot \boldsymbol{u} &= 0 \end{aligned} \tag{2.1}$$

Under the Boussinesq assumption that density fluctuations are small, the thermodynamic equation is written as equation (4) in the system above. The buoyancy is characterised by Potential Temperature, θ as $b = \frac{g\theta}{\theta_0}$. By also introducing the geopotential $\phi = \frac{p}{\rho_0}$, equations 2.1 are rewritten as

$$\begin{aligned} \frac{\mathrm{D}u}{\mathrm{D}t} - fv &= -\frac{\partial \phi}{\partial x} \\ \frac{\mathrm{D}v}{\mathrm{D}t} + fu &= -\frac{\partial \phi}{\partial y} \\ \frac{\mathrm{D}w}{\mathrm{D}t} &= -\frac{\partial \phi}{\partial z} + \frac{g\theta}{\theta_0} \\ \frac{\mathrm{D}\theta}{\mathrm{D}t} &= 0 \\ \nabla \cdot \boldsymbol{u} &= 0 \end{aligned} \tag{2.2}$$

where θ_0 and g denote initial potential temperature and acceleration due to gravity respectively.
$\frac{\mathrm{D}}{\mathrm{D}t} \equiv \frac{\partial}{\partial t} + u\frac{\partial}{\partial x} + v\frac{\partial}{\partial y} + w\frac{\partial}{\partial z}, \qquad \nabla \equiv \left(\frac{\partial}{\partial x}, \frac{\partial}{\partial y}, \frac{\partial}{\partial z}\right)$

Additionally if the hydrostatic approximation, that vertical acceleration is small

compared to gravity, so that, $\frac{\mathrm{D}w}{\mathrm{D}t} = 0$. Then,

$$\begin{aligned} \frac{\mathrm{D}u}{\mathrm{D}t} - fv &= -\frac{\partial \phi}{\partial x} \\ \frac{\mathrm{D}v}{\mathrm{D}t} + fu &= -\frac{\partial \phi}{\partial y} \\ -\frac{\partial \phi}{\partial z} + \frac{g\theta}{\theta_0} &= 0 \\ \frac{\mathrm{D}\theta}{\mathrm{D}t} &= 0 \\ \nabla \cdot \boldsymbol{u} &= 0 \end{aligned} \tag{2.3}$$

2.1.2 The Vertical Slice Model

To facilitate the study of frontogenesis a vertical slice model is introduced. In this report the vertical slice is defined as the $(x - z)$ plane. The domain considered is defined as, $\Gamma := [-L, L] \times [0, H]$. Perturbations to the leading-order fields are considered as functions of x, z and t only, whereas the leading order terms in θ and ϕ are functions of (y, z). Retaining the potential temperature gradient normal to the slice is crucial to the subsequent evolution of the front. Following the ideas of Yamazaki, 2017 [5] we introduce,

$$\begin{aligned} \theta &= \bar{\theta}(y, z) + \theta'(x, z, t) \\ \phi &= \bar{\phi}(y, z) + \varphi(x, z, t) \\ \boldsymbol{u} &= \bar{\boldsymbol{u}}(y, z) + \boldsymbol{u}'(x, z, t) \end{aligned} \tag{2.4}$$

With the background field for θ chosen as,

$$\bar{\theta} = -Cy \tag{2.5}$$

Where $\frac{\partial \theta}{\partial y} = -C$ is a constant, normal to the slice potential temperature gradient.

The background field for ϕ is chosen so that both background fields for θ and ϕ satisfy the third equation of 2.3,

$$-\frac{\partial \bar{\phi}}{\partial z} + \frac{g\bar{\theta}}{\theta_0} = 0$$

with the boundary condition $\phi = 0$ at $z = H/2$. This gives,

$$\bar{\phi} = -\frac{Cgy}{\theta_0}(z - H/2) \tag{2.6}$$

Comment: not here:

The Brunt-Väisälä frequency $N^2 = \frac{g}{\theta_0}\frac{\partial \theta}{\partial z}$ characterises the stratification of density in the slice.

To reach the vertical slice model we substitute the forms 2.4 with expressions for the background fields 2.5 and 2.6 into equations 2.3.

$$\begin{aligned}
\frac{\mathrm{D}u}{\mathrm{D}t} - fv &= -\frac{\partial}{\partial x}\left(\bar{\phi} + \varphi\right) \\
\frac{\mathrm{D}v}{\mathrm{D}t} + fu &= -\frac{\partial}{\partial y}\left(\bar{\phi} + \varphi\right) \\
0 &= \frac{\partial}{\partial z}\left(\bar{\phi} + \varphi\right) - \frac{g}{\theta_0}\left(\bar{\theta} + \theta'\right) \\
0 &= \frac{\partial}{\partial t}\left(\bar{\theta} + \theta'\right) + u\frac{\partial}{\partial x}\left(\bar{\theta} + \theta'\right) + v\frac{\partial}{\partial y}\left(\bar{\theta} + \theta'\right) + w\frac{\partial}{\partial z}\left(\bar{\theta} + \theta'\right) \\
0 &= \frac{\partial u}{\partial x} + \frac{\partial v}{\partial y} + \frac{\partial w}{\partial z}
\end{aligned} \tag{2.7}$$

By neglecting $\partial/\partial y$ terms except in background variables, after rearrangement the vertical slice equations are obtained as,

$$\begin{aligned}
\frac{\partial u}{\partial t} + u\frac{\partial u}{\partial x} + w\frac{\partial u}{\partial z} - fv &= -\frac{\partial \varphi}{\partial x} \\
\frac{\partial v}{\partial t} + u\frac{\partial v}{\partial x} + w\frac{\partial v}{\partial z} + fu &= -\frac{\partial \varphi}{\partial y} + \frac{Cg}{\theta_0}\left(z - H/2\right) \\
0 &= \frac{\partial \varphi}{\partial z} - \frac{g\theta'}{\theta_0} \\
0 &= \frac{\partial \theta'}{\partial t} + u\frac{\partial \theta'}{\partial x} - Cv + w\frac{\partial \theta'}{\partial z} \\
0 &= \frac{\partial u}{\partial x} + \frac{\partial w}{\partial z}
\end{aligned} \tag{2.8}$$

By redefining the material derivative operator as $\frac{\mathrm{D}}{\mathrm{D}t} \equiv \frac{\partial}{\partial t} + u\frac{\partial}{\partial x} + w\frac{\partial}{\partial z}$, and gradient operator $\nabla = \left(\frac{\partial}{\partial x}, \frac{\partial}{\partial z}\right)$

$$\begin{aligned}
\frac{\mathrm{D}u}{\mathrm{D}t} - fv &= -\frac{\partial \varphi}{\partial x} \\
\frac{\mathrm{D}v}{\mathrm{D}t} + fu - \frac{Cg}{\theta_0}\left(z - H/2\right) &= -\frac{\partial \varphi}{\partial y} \\
\frac{\partial \varphi}{\partial z} - \frac{g\theta'}{\theta_0} &= 0 \\
\frac{\mathrm{D}\theta'}{\mathrm{D}t} - Cv &= 0 \\
\nabla \cdot \boldsymbol{u} &= 0
\end{aligned} \tag{2.9}$$

2.1.3 The Geostrophic Momentum Approximation

To reach the final semi-geostrophic Eady model for frontogenesis the Geostrophic Momentum approximation is made. Developed by Hoskins, 1975 [3], where further detail can be found, the following section gives a brief summary of the key arguments.

Going back to equations 2.2. We consider an expansion in the Rossby number $\epsilon = U/fL$ where U and L are horizontal velocity and length scaled respectively. Expanding the momentum equations in 2.9 in leading-order (geostrophic) and first order (ageostrophic) terms in ϵ, so that,

$$\boldsymbol{u} = \boldsymbol{u_g} + \epsilon \boldsymbol{u_a} \qquad \varphi = \varphi_g + \epsilon \varphi_a$$

Acceleration terms are found to be $O(\epsilon)$ so that at the leading order the geostrophic balance is found to be,

$$f v_g = -\frac{\partial \varphi_g}{\partial x} \qquad -f u_g = -\frac{\partial \varphi_g}{\partial y} \tag{2.10}$$

Subsequent analysis as detailed in Hoskins 1975, [3] finds the prognostic equations for ageostrophic variables to be such that the momentum $\frac{\mathrm{D}u}{\mathrm{D}t}, \frac{\mathrm{D}v}{\mathrm{D}t}$ are replaced with their geostrophic counterparts $\frac{\mathrm{D}u_g}{\mathrm{D}t}, \frac{\mathrm{D}v_g}{\mathrm{D}t}$. Noting that in the vertical slice model $u_g = 0$ we find equations 2.8 with the geostrophic momentum approximation as

$$\begin{aligned} -f v_g + \frac{\partial \varphi}{\partial x} &= 0, \\ \frac{D v_g}{D t} + f u - \frac{C g}{\theta_0}(z - H/2) &= 0, \\ \frac{D \theta'}{D t} - C v_g &= 0, \\ \frac{\partial \varphi}{\partial z} - g\frac{\theta'}{\theta_0} &= 0, \\ \nabla \cdot \boldsymbol{u} &= 0. \end{aligned} \tag{2.11}$$

Comment: First equation is different - $-fv_g$ isn't $O(\epsilon)$??

Where, for convenience the subscript denoting ageostrophic variables has been dropped.

The corresponding energy integral given by [2] is,

$$E = \iint_\Gamma \frac{1}{2} v_g^2 - \frac{g\theta'}{\theta_0}(z - H/2)\,\mathrm{d}x\mathrm{d}z \tag{2.12}$$

Equations 2.11 form the basis of the subsequent investigation of frontogenesis in this report. They are to be solved over the domain $\Gamma = [-L, L] \times [0, H]$, with the periodic boundary conditions in x and the rigid-lid boundary condition $w = 0$ on $z = 0, H$.

The front formation seen later in the report is a consequence of a baroclinic instability introduced by Cullen 2006 [2] in the form of a perturbation to θ',

$$\theta' = \frac{N^2 \theta_0 z}{g} + B \sin\left(\pi \left(x/L + z/H\right)\right) \tag{2.13}$$

Comment: does this need including?

- **Key Scalings** It is worth noting that Eady's original model for baroclinic instability was developed under a quasi-geostrophic model, where $\epsilon = Fr \ll 1$ in contrast semi-geostrophic theory the assumes, $\epsilon \ll 1$ with $\epsilon < Fr$.

Chapter 3

The Frontogenesis Model as an Optimal Transport Problem

The semi-geostrophic equations have previously been rigorously analysed [3, 6, 7] and models subsequently developed to include momentum diffusion [8, 9]. The existence of smooth solutions for the Eady Model for frontogenesis 2.11 is shown in [10]. Perhaps one of the most exciting developments in the study of frontogenesis was the reformulation of the semi-geostrophic equations into a Monge-Ampère equation for mass transportation [11] **Comment: CHECK!**
. It is shown in [2] that a through a transformation to geostrophic co-ordinates as described in section 2.1.3 the energy integral can be viewed as the 'cost' in a moss transportation problem. This reformulation has allowed a deeper insight into the behaviour of the equations through numerical solutions developed from methods in computational geometry. In this chapter the arguments given in [2] are summarised to highlight the application of optimal transport theory to the Eady Model for frontogenesis 2.11. **Comment: smooth solutions only in geostrophic co-ordinates**

3.1 Transformation to Geostrophic Co-ordinates

To facilitate the implementation of the numerical scheme we will subsequently use to solve equations 2.11 we transform to geostrophic co-ordinate system first introduced by Hoskins [3] in the horizontal directions (x, y). The geostrophic co-ordinates describe the position of particles had they evolved under their geostrophic velocity. This transformation was later developed by Cullen [2] to include a transformation in terms of θ' in the vertical direction. The geostrophic transformation

$\Phi : (x, z) \to (X, Z)$

$$X = x + \frac{v_g}{f}, \qquad Z = \frac{g\theta'}{f^2\theta_0} \tag{3.1}$$

By defining

$$P = \frac{1}{2}x^2 + \frac{1}{f^2}\varphi \tag{3.2}$$

It is clear that,

$$\nabla P = \left(x + \frac{1}{f^2}\frac{\partial\varphi}{\partial x}, \frac{1}{f^2}\frac{\partial\theta'}{\partial z}\right) \quad = \left(x + \frac{v_g}{f}, \frac{g\theta'}{f^2\theta_0}\right)$$

So that upon substitution from the first and fourth equations in 2.11 we find,

$$\nabla P = (X, Z) \tag{3.3}$$

By noting that,

$$\frac{\mathrm{D}X}{\mathrm{D}t} = \frac{\mathrm{D}x}{\mathrm{D}t} + \frac{1}{f}\frac{\mathrm{D}v_g}{\mathrm{D}t} = u + \frac{1}{f}\frac{\mathrm{D}v_g}{\mathrm{D}t}, \qquad \frac{\mathrm{D}Z}{\mathrm{D}t} = \frac{g}{f^2\theta_0}\frac{\mathrm{D}\theta'}{\mathrm{D}t}$$

the momentum equations from 2.11 are transformed into geostrophic co-ordinates as

$$\frac{\mathrm{D}X}{\mathrm{D}t} - \frac{Cg}{f\theta_0}(z - H/2) = 0, \qquad \frac{\mathrm{D}Z}{\mathrm{D}t} - \frac{Cg}{f\theta_0}(X - x) = 0, \tag{3.4}$$

It is also shown in [2] that the continuity equation holds in geostrophic co-ordinates. with $\boldsymbol{U} = \frac{Cg}{f\theta_0}(z - H/2, X - x)$ Putting together equations 3.2, 3.3, 3.4 the Eady Model in geostrophic co-ordinates is

$$\begin{aligned} \frac{\mathrm{D}X}{\mathrm{D}t} - \frac{Cg}{f\theta_0}(z - H/2) &= 0 \\ \frac{\mathrm{D}Z}{\mathrm{D}t} - \frac{Cg}{f\theta_0}(X - x) &= 0, \\ P = \frac{1}{2}x^2 + \frac{1}{f^2}\varphi, & \\ \nabla P = (X, Z) & \\ \nabla \cdot \boldsymbol{U} = 0 & \end{aligned} \tag{3.5}$$

The corresponding energy integral given by transforming the Energy 3.6 with 3.1 is,

$$E = f^2 \iint \frac{1}{2}(X - x)^2 - Z(z - H/2)\,\mathrm{d}x\mathrm{d}z \tag{3.6}$$

3.2 Energy Minimisation as an Optimal Transportation Problem

It is shown in [2] and references therein that the hydrostatic and geostrophic balances in the Semi-geostrophic equations characterise the solution as an Energy minimisation problem. In geostrophic co-ordinates, Theorem 3.3 from [2] the condition to minimise the energy 3.6 is that the function P is convex. In this section we show that this can be reformulated to take the form of an optimal transport problem with quadratic cost. This amounts to the solution of 3.5 as finding (X, Z) which minimise the energy and subsequently finding their time evolution using 3.5.

3.2.1 Finding an Inverse Transformation

Consider an initial set of points in geostrophic space (X, Z). To find the trajectory of points in geostrophic space and consequently to solve 3.5 requires the corresponding values (x, z). This requires the existence of a unique inverse to the transform 3.1. Following [2], the function $R(X, Z)$ is defined as,

$$R(X, Z) = x(X, Z)X + z(X, Z)Z - P(x, y, z)$$

To rewrite the energy integral 3.6 in geostrophic co-ordinates requires the jacobian of the inverse transformation $\Phi^{-1} : (X, Z) \to (x, z)$,

$$\sigma(X, Z) = \frac{\partial x}{\partial X}\frac{\partial z}{\partial Z} - \frac{\partial z}{\partial X}\frac{\partial x}{\partial Z} \tag{3.7}$$

Noting that,

$$\frac{\partial R}{\partial X} = x + X\frac{\partial x}{\partial X} + Z\frac{\partial z}{\partial X} - \frac{\partial P}{\partial x}\frac{\partial x}{\partial X} - \frac{\partial P}{\partial x}\frac{\partial z}{\partial X}$$

Similarly,

$$\frac{\partial R}{\partial Z} = X\frac{\partial x}{\partial Z} + z + Z\frac{\partial z}{\partial Z} - \frac{\partial P}{\partial Z}\frac{\partial x}{\partial Z} - \frac{\partial P}{\partial Z}\frac{\partial z}{\partial Z}$$

Using $\nabla P = (X, Z)$, we find,

$$\nabla_{(X,Z)} R = \left(\frac{\partial R}{\partial X}, \frac{\partial R}{\partial Z}\right) = (x, z) \tag{3.8}$$

This is convenient as it allows us to rewrite 3.7 as,

$$\sigma(X, Z) = \frac{\partial^2 R}{\partial X^2}\frac{\partial^2 R}{\partial Z^2} - \frac{\partial^2 R}{\partial X Z}\frac{\partial^2 R}{\partial Z X} = \det(Hess\ R) \tag{3.9}$$

As stated in [2] this is a form of the classical **Monge Ampère equation** for a given $\sigma(X, Z)$. Paired with the boundary condition that the fluid in physical co-ordinates

stays within the domain,Γ, (ie) $(x,z) = \nabla_{(X,Z)} R \in \Gamma$. This can be expressed as,

$$\iint_{\mathbb{R}^2} \sigma\,(X,Z)\ dXdZ = \iint_{\Gamma} dxdz \tag{3.10}$$

Physically this is equivalent to conservation of volume for all time so that in a similar statement the mass continuity equation in classical fluid mechanics, with $\nabla \cdot U = 0$,

$$\frac{\mathrm{D}_{(X,Z)}\sigma}{\mathrm{D}t} = \frac{\partial \sigma}{\partial t} + \frac{\partial U}{\partial X}\frac{\partial \sigma}{\partial X} + \frac{\partial W}{\partial Z}\frac{\partial \sigma}{\partial Z} \tag{3.11}$$

This gives a prognostic equation for $\sigma(X,Z)$ **Comment: include full system of equations?**

3.2.2 The Monge Ampère equation and Optimal Transportation

Again giving an overview of the arguments in [2] we show how the Monge Ampère equation 3.9 can be solved as an optimal transport problem.

The density σ can be seen to define a measure on $\mathbb{R}^2$, where the measure of the set $A \subseteq \mathbb{R}^2$ is defined an $\nu(A) = \iint_A \sigma(X,Z)\, dXdZ$. On the domain γ in physical coordinates (x,z) we consider the scaled Lebesgue measure $\mu(\gamma) = \mathrm{Area}(\Gamma)^{-1} \iint_\gamma dxdz$, where $\gamma \subseteq \Gamma$ and $\mathrm{Area}(\Gamma) = \iint_\Gamma dxdz$. Considering mappings $s : \mathbb{R}^2 \to \Gamma$ that preserve measure so that if $\gamma = s(A)$, we have $\nu(A) = \mu(\gamma)$. The reader is referred to [12] for a rigorous explanation of concepts in measure theory.

With this in mind, given the mapping $s : \mathbb{R}^2 \to \Gamma$ the energy is defined in [2] as the following,

$$E = f^2 \iint \frac{1}{2}\,(X - \tilde{x})^2 - Z\,(\tilde{z} - H/2)\,\sigma\ \mathrm{d}X\mathrm{d}Z \tag{3.12}$$

where $(\tilde{x},\tilde{z}) = s(X,Z)$. The solution for equations 3.5 is then encapsulated in Theorem (3.4) of [2] which says that the condition for the energy to be minimised is that,

$$s(X,Z) = \nabla R \tag{3.13}$$

with condition 3.10 as above. **Comment: Convexity of R?**

We now put this into the context of the discrete problem which will be susequently

solved in the implementation of the optimal transport solver from [13]. In this case we consider Γ to be a partition into N 'fluid parcels' of equal volume. For convenience we consider the case where the total volume of Γ is $\iint_\Gamma \ dxdz = 1$.

The density σ is defined discretely for N points $\boldsymbol{Y}_i = (X_i, Z_i)$ in geostrophic space as $\sigma(X,Y) = \sum_{i=1}^{N} \frac{1}{N}\delta\left(\boldsymbol{Y} - \boldsymbol{Y}_i\right)$. Note, this also gives $\iint_{\mathbb{R}^2} \sigma\left(X,Z\right) \ dXdZ = 1$. The problem in this case becomes finding a map $s : \mathbb{R}^2 \to \Gamma$ such that the energy,

$$E = f^2 \iint \frac{1}{2}\left(X_i - \tilde{x}\right)^2 - Z_i\left(\tilde{z} - H/2\right)\sigma \ \mathrm{d}X\mathrm{d}Z \tag{3.14}$$

is minimised and such that the volume of the associated 'fluid parcels', (ie) the sets $A_i = s^{-1}(X_i, Z_i)$ is preserved. Figure 3.1 illustrates such a transformation. Theorem (3.11) from [2] proves the existence of such a map for the density σ. The final piece

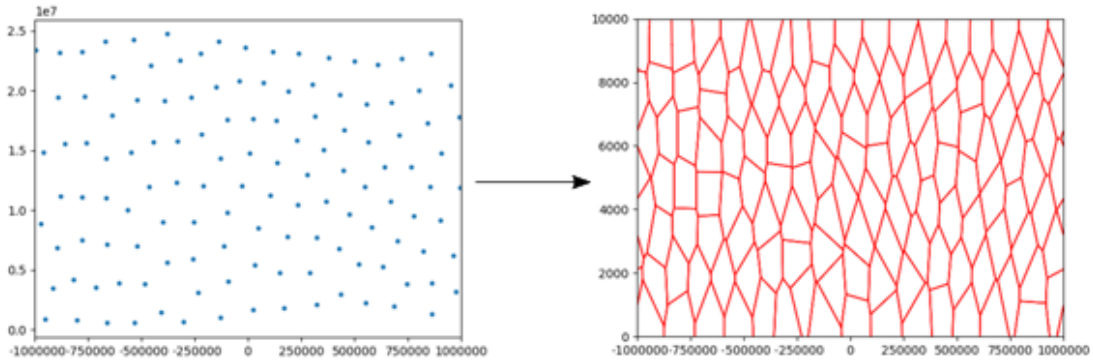

Figure 3.1: Figure illustrating a map from geostrophic points to fluid 'parcels' that preserves volume.

is in the formulation of the solution of the semi-geostrophic equations as an optimal transport problem uses Theorem (3.16) from [2]. We restate this using the notation above.

Theorem 3.2.1. *Given probability measures σ, μ with bounded supports $\Sigma \subset \mathbb{R}^2$, $\Gamma \subset \mathbb{R}^2$. There exist optimal maps $t : \Sigma \to \Gamma$ and $t^{-1} : \Gamma \to \Sigma$ which are inverses and minimise a quadratic cost function given by*

$$\iint_{\mathbb{R}^2} \left(\frac{1}{2} f^2 |\boldsymbol{Y} - t(\boldsymbol{Y})|^2\right) \sigma \ dXdZ$$

Furthermore, these maps are unique up to sets of measure zero.

The reader is referred to [12] for a detailed discussion of measure theory and zero measure sets.

The proof is given in [2] and is a culmination of the results stated above. Γ is clearly bounded by definition and Σ is a set of finite points it too is also bounded. Furthermore since *sigma* and μ are defined so that their integrals over Σ and Γ are unity, they are probability measures over their respective domains.

It remains to show that the minimisation of the quadratic cost function is equivalent to minimising the energy. For this we transform the cost function to physical co-ordinates as,

$$\iint_{\mathbb{R}^2} \left(\frac{1}{2} f^2 |t^{-1}(\boldsymbol{y}) - \boldsymbol{y}|^2 \right) \, dxdz$$

The following Lemma proves this to be equivalent to minimising the energy given by 3.6.

Lemma 3.2.2. *Minimising the Energy integral given by,*

$$E = f^2 \iint_\Gamma \frac{1}{2} (X - x)^2 - Z (z - H/2) \, dxdz$$

is equivalent to minimising the quadratic cost integral given by,

$$E = f^2 \iint_\Gamma \frac{1}{2} \left((X - x)^2 + (Z - z)^2 \right) dxdz$$

Proof. We begin by noting that the difference in the energy integrals is in the potential energy term, so it suffices to show that the minimisation of these terms is equivalent. Expanding to see,

$$\iint_\Gamma -Z (z - H/2) \, \mathrm{d}x\mathrm{d}z = \iint_\Gamma -Zz + \frac{ZH}{2} \mathrm{d}x\mathrm{d}z \tag{3.15}$$

$$\iint_\Gamma \frac{1}{2} (Z - z)^2 \, \mathrm{d}x\mathrm{d}z = \iint_\Gamma \frac{1}{2} Z^2 - Zz + \frac{1}{2} z^2 \, \mathrm{d}x\mathrm{d}z \tag{3.16}$$

Recalling that Z is a function of (x, z), the treatment of terms with this variable need to be considered carefully. As both 3.15 and 3.16 contain $\iint_\Gamma -Zz$, this can also be omitted from consideration.

Considering $\iint_\Gamma \frac{1}{2} Z^2 \mathrm{d}x\mathrm{d}z$. Given a partition of Γ into N cells up to zero measure sets, so that $\Gamma = \bigcup_{i=1}^N c_i$. Applying the transform $\Phi : (x, z) \to (X, Z)$, and using that the transform maps cells in physical space to points in geostrophic space

$$\sum_{i=1}^N \iint_{c_i} \frac{1}{2} Z^2 \mathrm{d}x\mathrm{d}z = \sum_{i=1}^N \iint_{\Phi(c_i)} \frac{1}{2} Z^2 \sigma(X, Z) \, \mathrm{d}X\mathrm{d}Z$$

But since $\sigma(X,Z) = \sum_{i=1}^{N} \frac{1}{N}\delta(\boldsymbol{Y} - \boldsymbol{Y_i})$

$$\implies \sum_{i=1}^{N} \frac{1}{N}\frac{1}{2}Z_i^2$$

However this is a fixed value. Similar arguments give that,

$$\sum_{i=1}^{N} \iint_{c_i} \frac{HZ}{2}\,\mathrm{d}x\mathrm{d}z = \sum_{i=1}^{N} \frac{HZ_i}{2}$$

Hence, the minimisation of 3.15 and 3.16 is equivalent. □

To summarise the results of this Chapter, we began by transforming the semi-geostrophic equations to geostrophic co-ordinates. In this setting finding the solution to equations 3.5 was shown to amount to an energy minimisation problem with the energy being defined by 3.6. Through the use of the Jacobian for the transformation σ and an appropriately defined function $R(X,Z)$ we were able to show this energy minimisation to be the solution of a Monge Ampére equation. Subsequently, through the use of probability measures this was shown to be equivalent to a discrte optimal transport problem with quadratic cost. Finally by showing the equivalence of minimising energy to minimising the quadratic cost function the problem is formulated as an optimal transport problem. **Comment: tie energy minimisation to Monge ampere equation/optimal transport**

Chapter 4

Semi-discrete Optimal Transport

The Damped Newton algorithm, hereafter DA, developed by Mérigot et al. [13] solves a semi-discrete Monge-Ampère type optimal transport problem. It's efficiency in exploiting the properties of sparse matrices and linear convergence [13] make it practical for implementation in the solution for equations 3.5. Further detail describing the application of the algorithm in the solution to the Eady Model is given in chapter 5. In this chapter an overview of semi-discrete optimal transport is given using definitions given in [14, 13] as well as a comparison to the energy minimisation to which it is applied. A rigorous proof of the formulation of 2.11 as a Monge-Ampère type optimal transport problem is given in Cullen, 2006 [2].

4.1 Semi-discrete Optimal Transport

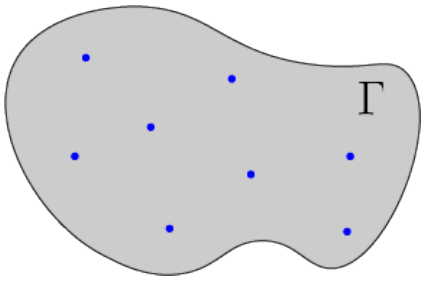

Figure 4.1: A discrete (target) set $Y \subseteq \mathbb{R}^2$ represented by blue points in a compact domain (source) $\Gamma \subseteq \mathbb{R}^2$

Optimal transport problems describe the problem of finding a map between two sets, a target set and a source set, each with an associated density, in such a way that the "cost" associated with the mapping is minimised. In semi-discrete optimal transport the target set is a finite set.

In Kitagawa et al. [14] a wonderful analogy with travel distance to bakeries in

a city is made, where the source set is considered as a city and the discrete target set is the locations of bakeries in the city. In this report the problem will be explained in the context in which it will subsequently be implemented. Namely, the source set is the domain Γ, the physical space described in section 3 and the target set, the set of points in geostrophic space. The optimal transport problem finds a partition of the domain, up to sets of measure zero, such that every point in a region of the partion is closest to the point at the centre of that region. In this analogy the cost being minimised is the travel distance to the point $\boldsymbol{Y}_i$, $c(\boldsymbol{x}, \boldsymbol{Y}_i) = \|\boldsymbol{x} - \boldsymbol{Y}_i\|^2$, where $\boldsymbol{x} \in \Gamma$. This is illustrated in figure 4.2 below

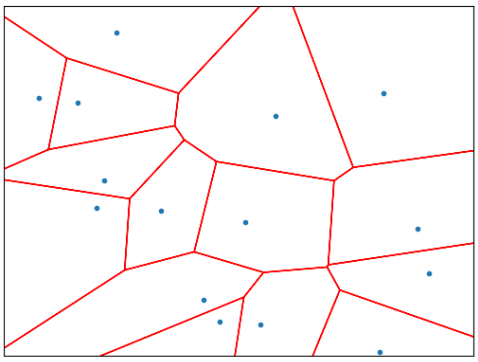

Figure 4.2: The image showing how a domain would be divided into areas based on minimising distance to the blue points. This is a Voronoi tesselation of the domain Γ based on the minimisation of $c(\boldsymbol{x}, \boldsymbol{Y_i})$

To put this into a more rigorous mathematical setting, given a domain $\Gamma \subseteq \mathbb{R}^2$ and discrete set of N points $Y = \{\boldsymbol{Y}_i = (X_i, Z_i), \quad 1 \leq i \leq N\} \subset \mathbb{R}^2$,

Definition 4.1.1. Source measure
Defined on the domain Γ. $\mu(A) = \text{Area}(\Gamma)^{-1} \int_A \, dxdz$, $A \subseteq \Gamma$. Note this defines a probability measure with a uniform probability density on Γ.

Definition 4.1.2. Target measure
Defined on $\mathbb{R}^2$ $\sigma((X, Z)) = \sum_{i=1}^{N} \sigma_i \delta\left(\boldsymbol{Y} - \boldsymbol{Y}_i\right)$, with finite support on $\mathbb{R}^2$. Note this defines a discrete probability measure when $\sigma(\mathbb{R}^2) = 1$, for appropriate choice of σ_i.

Definition 4.1.3. Voronoi Cells
The regions enclosed by the red lines and boundaries of the domain in 4.2 are defined as Voronoi cells, $\text{Vor}(\boldsymbol{Y}_i) := \{\boldsymbol{x} \in \Gamma \text{ st } \forall\, Y_j \in Y \; c(\boldsymbol{x}, \boldsymbol{Y}_i) \leq c(\boldsymbol{x}, \boldsymbol{Y}_j)\}$. The diagram is referred to as a Voronoi tesselation.

Definition 4.1.4. Transport map

$T : \Gamma \to Y$ between the source measure μ and the target measure on Y, μ if $T_{\#}\mu = \sigma$.

Definition 4.1.5. Pushforward of a measure μ by a map $T : \Gamma \to Y$ is $T_{\#}\mu = \sum_{\boldsymbol{Y}_i \in Y} \mu\left(T^{-1}(\boldsymbol{Y}_i)\right) \delta(\boldsymbol{Y} - \boldsymbol{Y}_i)$, the sum of the measures of the sets mapped to the points $\boldsymbol{Y}_i$ under T

From these definitions we can see that the optimal transport map is given by,

$$T(\boldsymbol{x}) = \arg\min_{\boldsymbol{Y}_i \in Y} \left(c(\boldsymbol{x}, \boldsymbol{Y}_i)\right) \iff \sigma(\boldsymbol{Y}_i) = \mu\left(\mathrm{Vor}(\boldsymbol{Y}_i)\right) \tag{4.1}$$

4.2 Laguerre Cells and the Inclusion of weights

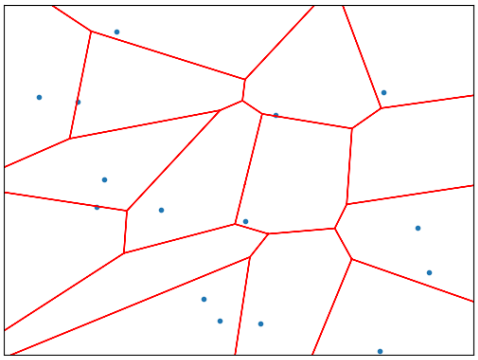

Figure 4.3: Given a uniform source and target density the Laguerre diagram produced by finding weights using DA for optimal transport

Considering again figure 4.2 it is clear that if the density across the domain Γ is uniform the distribution of area corresponding to each bakery is certainly not. For example, the Voronoi cells at the top right of the diagram in figure 4.2 are much larger in area than those in the centre of the diagram. This raises the problem of finding a way to create a partition such that each cell has the same area. This is done by introducing an additional "weight" argument to the cost. We denote the weights by $\psi_i = \psi\left(\boldsymbol{Y}_i\right) \in \mathbb{R}$. In the case of the bakeries the weights might represent the price of bread at a specific bakery. For this we introduce the notion of Laguerre cells.

Definition 4.2.1. Laguerre Cells
The regions enclosed by the red lines and boundaries of the domain in figure 4.3, $\mathrm{Lag}_{\boldsymbol{Y}_i}(\psi) := \{\boldsymbol{x} \in \Gamma \text{ st } \forall\ \boldsymbol{Y}_j \in Y\ c(\boldsymbol{x}, \boldsymbol{Y}_i) + \psi(\boldsymbol{Y}_i) \leq c(\boldsymbol{x}, \boldsymbol{Y}_j) + \psi(\boldsymbol{Y}_j)\}$

In this case, the optimal transport map is given by
$T_\psi : x \to \mathrm{argmin}_i \|x - y_i\|^2 + \psi_i$, where ψ_i is a family of weights on Y [13].

The problem is then finding the weights ψ_i associated to the points $\boldsymbol{Y}_i$ such that $\mu(\text{Lag}_{\boldsymbol{Y}_i}(\psi)) = \sigma(\boldsymbol{Y}_i) = \sigma_i$. The Damped Newton's Algorithm from Mérigot, Meyron and Thibert (2017) [13] finds such ψ_i.

Supposing that both the source density and target density are uniform, (ie) in definition 4.1.2 the Laguerre cells as found by the DA code developed in [13] are shown in figure 4.3. The Laguerre diagram highlights the fact that the densities are both specified to be uniform probability densities. In figure 4.2 the target density was not specified. This means that points are not necessarily interior to their corresponding Laguerre cells, however the cells have equal area. The cells in this case are the Laguerre cells defined above, and the weights that define the optimal transport map was found by [13] as

$$T(x) = \arg\min_{\boldsymbol{Y}_i \in Y} \left(c(\boldsymbol{x}, \boldsymbol{Y}_i) + \psi_i\right)$$

For the remainder of this report we will consider cases where both the source density and target density are uniform and the quadratic cost function is,

$$c(\boldsymbol{x}, \boldsymbol{Y}_i) = \|\boldsymbol{x} - \boldsymbol{Y}_i\|^2$$

4.3 Applying semi-discrete optimal transport to solving the semi-geostrophic equations

As shown in [2] equations 2.11 can be recast as an optimal transport problem using the transformation to geostrophic co-ordinates introduced by Hoskins [3]. In this section we outline how DA is applied to equations 2.11.

The optimal transport problem considered in the frontogenesis problem is the minimisation of the energy, restated from equation 3.6

$$E = f^2 \iint \frac{1}{2}(X - x)^2 - Z\,(z - H/2)\,\mathrm{d}x\mathrm{d}z \tag{4.2}$$

as shown by Lemma 3.2.2 this is equivalent to minimising 3.2.2,

$$E = \frac{f^2}{2} \iint \left((X - x)^2 + (Z - z)^2\right)\mathrm{d}x\mathrm{d}z \tag{4.3}$$

Considering the geostrophic co-ordinates as the target set of finite set of points for the optimal transport problem from the domain $\Gamma = [-L, L] \times [0, H]$. The DA Algorithm finds the weights such that the area of each Laguerre cell is preserved.

Physically, this amounts to the condition that the volume is conserved.

4.4 Extension for Periodic Boundary Conditions

As stated in Chapter 2 in the model for frontogenesis boundary conditions consider periodicity in x. This must be accounted for in the implementation of the Damped Newton Algorithm.

This inclusion of periodic boundary conditions allows Laguerre cells to cover areas over the right and left boundaries. This means that the Laguerre edges must be continuous across the boundaries if copies of the Laguerre diagram were placed on each boundary. The Laguerre cells must have the same mass, for example, in figure 4.4 below the top right cell extends to the left of the domain. The sum of the areas of each component of the cell must be the same as a cell in the centre of the diagram. The area of each cell remains the same as in 4.3 however the boundaries of the Laguerre cells are continuous across the left and right boundaries of the domain.

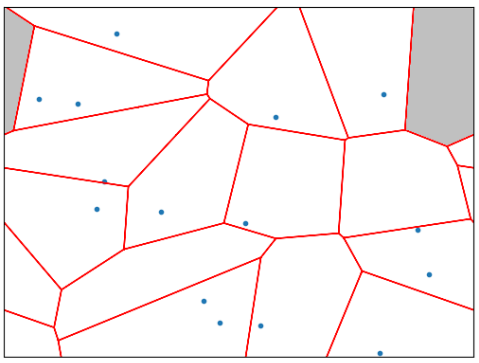

Figure 4.4: The solution to the optimal transport of the same points shown in figure 4.3, however with the density initialised with periodic boundary conditions in x. The area shaded in grey represents a single Laguerre cell.

4.4.1 Definitions of Mass with Periodic Boundary Conditions

Comment: include the definition of mass of a cell and a better written description of the partition given by a laguerre diagram (tesselation/zero measure sets)

Comment: include definition of the fundamental domain

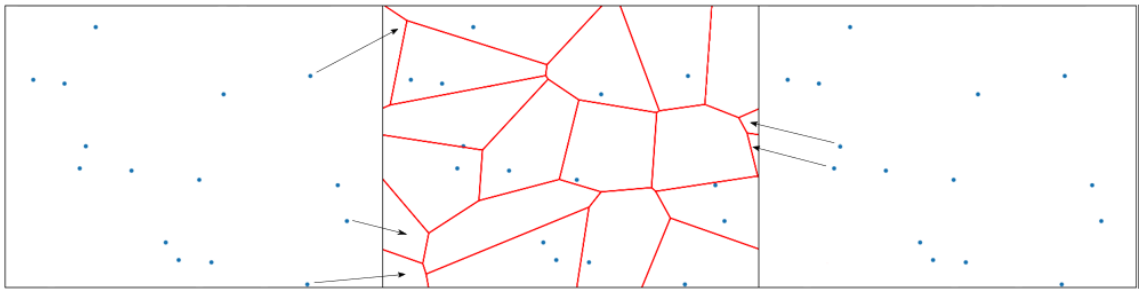

Figure 4.5: The image above shows how the Laguerre diagram for periodic boundary conditions is created with 'ghost' points on either side of the domain. Arrows show where ghost points contribute to Laguerre cells of positive mass in the domain Γ

4.4.2 Mapping to the Fundamental Domain

Under the geostrophic transformation 3.1 and also in time-stepping points in geostrophic space it is possible for points to travel exterior the boundaries of the domain Γ. In the x direction the boundary conditions imposed are periodic. If points are mapped so that their x-co-ordinates are exterior to the interval $[-L, L]$, they can be mapped to the domain Γ, the 'fundamental domain', using the periodicity, without affecting the result. **Comment: better phrasing please**

In fact, in the implementation of DA this is necessary at every time step to ensure that the mass of cells remains positive. This is implemented by the function 'to_fundamental_domain' adapted from DA [15] to treat periodic boundary conditions in x. An example of this is shown in figure 4.6 below, where the fundamental domain being considered is $[0, 1] \times [0, 1]$.

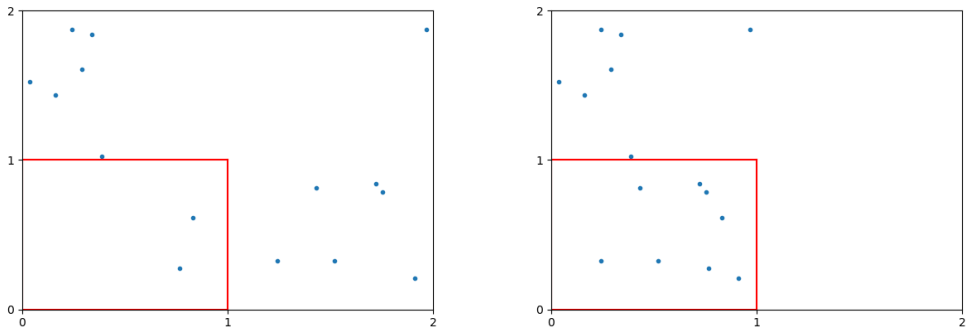

(a) (b)

Figure 4.6: Plots of a random set of points initialised in $[0, 2] \times [0, 2]$ before (a) and after (b) being mapped to the fundamental domain $[0, 1] \times [0, 1]$

To explain this rigorously, we consider the domain described by $[x_0, y_0] \times [x_1, y_1]$. Since we are only considering periodic boundary conditions in x, only the x co-ordinates will be mapped.

The mapping is performed by first finding the distance of the point from the left boundary of the domain as a ratio of the width of the domain. This is then added to left bound to give a value for x, $\tilde{x}$ that is in the fundamental domain.

$$X = x - \left\lfloor \frac{x - x_0}{x_1 - x_0} \right\rfloor$$
$$\tilde{x} = x_0 + (x_1 - x_0)X$$

This is implemented as: **Comment: insert to_fundamental_domain code**

Chapter 5

A Numerical Solution to the Eady Model for Frontogenesis

In this section the numerical implementation including the use of the Damped Newton Algroithm developed by [13] is explained in detail. Restating the problem, we are solving the semi-geostrophic equations 2.11 over the domain $\Gamma := [-L, L] \times [0, H]$.

$$\begin{aligned} -fv_g + \frac{\partial \varphi}{\partial x} &= 0, \\ \frac{Dv_g}{Dt} + fu - \frac{Cg}{\theta_0}(z - H/2) &= 0, \\ \frac{D\theta'}{Dt} - Cv_g &= 0, \\ \frac{\partial \varphi}{\partial z} - g\frac{\theta'}{\theta_0} &= 0, \\ \nabla \cdot \boldsymbol{u} &= 0. \end{aligned}$$

With boundary conditions:

- Rigid lid condition $w = 0$ on $z = 0, H$
- Periodic boundary conditions in x

Together with a baroclinic instability described by 2.13 as

$$\theta' = \frac{N^2 \theta_0 z}{g} + B \sin\left(\pi \left(x/L + z/H\right)\right) \tag{5.1}$$

The steps involved in solving the Eady Model for frontogenesis described above are detailed below,

Step 1 Initialise a set of points in physical space

Step 2 Transform physical points to Geostrophic space using the co-ordinate transformation given in 3.1, and map to fundamental domain Γ.

Step 3 Given the points in geostrophic space the weights which define the Laguerre

cells in the physical domain are calculated using the Damped Newton Algorithm.

Step 4 The equations are now time stepped from the transformed momentum equations 3.5

$$\frac{\mathrm{D}X_n}{\mathrm{D}t} - \frac{Cg}{f\theta_0}(\tilde{z}_n - H/2) = 0$$
$$\frac{\mathrm{D}Z_n}{\mathrm{D}t} - \frac{Cg}{f\theta_0}(X_n - \tilde{x}_n) = 0$$

Where X_n, Z_n represent the geostrophic points at the current time step, and $\tilde{x}_n, \tilde{z}_n$ represent the centroids of the Laguerre cells. In this project both a Forward-Euler scheme and Heun's method have been used for time-stepping.

Step 5 The geostrophic points are now replaced with X_{n+1}, Z_{n+1} and steps 3 and 4 are repeated until the final time is reached.

5.1 Initialisation of Points in Geostrophic Space

Given a finite set of equidistant points in the physical domain Γ, the points are transformed to geostrophic space using

$$X = x + \frac{v_g}{f}, \qquad Z = \frac{g\theta'}{f^2\theta_0} \tag{5.2}$$

This requires the form of θ' given by 2.13 from this v_g can be deduced using the following equations from 2.11,

$$\begin{aligned} \frac{\partial\varphi}{\partial z} - \frac{g\theta'}{\theta_0} &= 0 \\ \frac{\partial\varphi}{\partial x} - fv_g &= 0 \end{aligned} \tag{5.3}$$

using the boundary condition $\int_0^H \varphi(x,z)\,\mathrm{d}z = 0$ Integrating the first equation in z,

$$\frac{\partial\varphi}{\partial z} = \frac{g\theta'}{\theta_0} = N_0^2 z + \frac{Bg}{\theta_0}\sin\left(\pi\left(\frac{x}{L} + \frac{z}{H}\right)\right)$$
$$\varphi = \frac{N_0^2 z^2}{2} - \frac{BgH}{\theta_0\pi}\cos\left(\pi\left(\frac{x}{L} + \frac{z}{H}\right)\right) + F(x)$$

Applying the boundary condition to determine $F(x)$,

$$\int_0^H \varphi\,\mathrm{d}z = \left[\frac{N_0^2 z^3}{6} - \frac{BgH^2}{\theta_0\pi^2}\sin\left(\pi\left(\frac{x}{L} + \frac{z}{H}\right)\right) + F(x)z\right]_0^H = 0$$

Using $\sin\left(\frac{\pi x}{L}+\pi\right) = -\sin\left(\frac{\pi x}{L}\right)$,

$$0 = \frac{N_0^2 H^3}{6} - \frac{BgH^2}{\theta_0 \pi^2}\sin\left(\frac{\pi x}{L}+\pi\right) + \frac{BgH^2}{\theta_0\pi^2}\sin\left(\frac{\pi x}{L}\right) + F(x)H$$
$$0 = \frac{N_0^2 H^3}{6} + \frac{2BgH^2}{\theta_0 \pi^2}\sin\left(\frac{\pi x}{L}\right) + F(x)H$$

This gives $F(x)$ as,

$$F(x) = -\frac{N_0^2 H^2}{6} - \frac{2BgH^2}{\theta_0\pi^2}\sin\left(\frac{\pi x}{L}\right)$$

and consequently φ as,

$$\varphi(x,z) = \frac{N_0^2 z^2}{2} - \frac{BgH}{\theta_0\pi}\cos\left(\pi\left(\frac{x}{L}+\frac{z}{H}\right)\right) - \frac{N_0^2H^2}{6} - \frac{2BgH}{\theta_0\pi^2}\sin\left(\frac{\pi x}{L}\right) \tag{5.4}$$

Using the second of equations 5.3 v_g is found as,

$$v_g = \frac{BgH}{f\theta_0 L}\cos\left(\pi\left(\frac{x}{L}+\frac{z}{H}\right)\right) - \frac{2BgH}{f\theta_0\pi}\sin\left(\frac{\pi x}{L}\right) \tag{5.5}$$

Together with θ' given by 2.13 this expression for v_g can be used to determine X and Z in geostrophic co-ordinates through the transform 5.2.

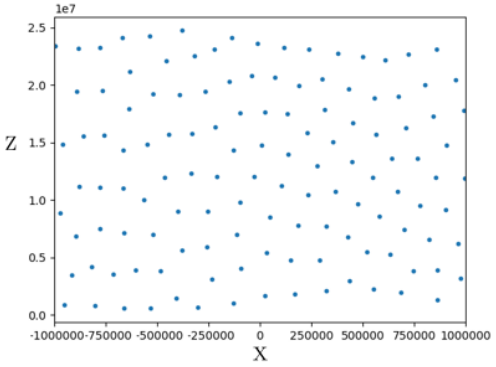

Figure 5.1: Plot of points in geostrophic space, transformed from a random set of points in $\Gamma := [-L, L] \times [0, H]$ using 3.1 with v_g as defined in 5.5

5.2 Choice of Initial Weights

The Laguerre diagram of this set of points shown in figure 5.1 with zero weights would define Laguerre cells exterior to Γ. These cells will have zero "mass "in the domain Γ. Physical intuition tells us that given the rigid lid and periodic boundary conditions points would physically not be able to leave the domain. However,

thinking of fluid particles as the centroids of Laguerre cells, a cell outside the domain would represent a fluid particle on the exterior of the domain. This also poses a problem with respect to the implementation of DA, as emphasised in [13], as it requires $\mu\left(\text{Lag}_{y_i}(\psi)\right)$ to be a monotonic function of $\psi = (\psi(y_1), ..., \psi(y_N))$ where N is the number of points initialised in Γ. According to [13] this occurs near points where the Laguerre cells contain positive mass over Γ.

Fortunately, a solution is provided in [13]. Proposition 25 in the paper proves that if the initial weights are given by,

$$\psi_i^0 = d\left(\boldsymbol{Y}_i, \Gamma\right)^2$$

where $\boldsymbol{Y}_i = (X_i, Z_i)$ are the points in geostrophic space. Since the domain is rectangular vertical distance from the point to the upper or lower boundary of the domain. The boundaries, given by $z = 0$ and $z = H$ are also perturbed to guarantee strict positivity of the mass of the Laguerre cells,

$$\psi_i^0 = \begin{cases} \left(Z_i - 0.9H\right)^2, & Z_i > 0.9H \\ \left(Z_i - 0.1H\right)^2, & Z_i < 0.1H \end{cases} \tag{5.6}$$

Comment: Address disparity with paper '-' sign - convention used in paper for finding Laguerre cells different to code?

The Damped newton algorithm, DA, is initialised with the the geostrophic points and weights given by 5.6. The algorithm outputs weights that give Laguerre cells with equal mass over the periodic domain.

5.3 Time Stepping

Once the initial points and weights have been set up, it remains to find the geostrophic points at the next time step, using equations 3.5.

5.3.1 Forward-Euler Scheme

The numerical solution to equations 2.11 developed follows a Lagrangian framework, thus it is justified to treat the material derivative $\frac{\mathrm{D}}{\mathrm{D}t}$ as a full derivative $\frac{\mathrm{d}}{\mathrm{d}t}$, in this sense we will develop prognostic scheme using the equations,

$$\begin{aligned} \frac{\mathrm{d}X}{\mathrm{d}t} - \frac{Cg}{f\theta_0}\left(\tilde{z} - H/2\right) = 0 \\ \frac{\mathrm{d}Z}{\mathrm{d}t} - \frac{Cg}{f\theta_0}\left(X - \tilde{x}\right) = 0 \end{aligned}$$

Applying a Forward-Euler scheme [16] for time-stepping given by,

$$\begin{aligned} t^{n+1} &= t^n + h \\ Z_i^{n+1} &= Z_i^n + \frac{hCg}{f\theta_0}\left(X_i^n - \tilde{x}_i^n\right) \\ X_i^{n+1} &= X_i^n + \frac{hCg}{f\theta_0}\left(\tilde{z}_i^n - H/2\right) \end{aligned} \tag{5.7}$$

where $\tilde{x}_i^n, \tilde{z}_i^n$ represent the centroids of the Laguerre cells given by equations 5.8 using X_i^n, Z_i^n and corresponding weights given by the optimal transport algorithm (DA),

$$\tilde{x}_i^n = \frac{\int_{\mathrm{Lag}_{\boldsymbol{Y}_i^n}(\psi)} x \, \mathrm{d}x\mathrm{d}z}{\int_{\mathrm{Lag}_{\boldsymbol{Y}_i^n}(\psi)} \mathrm{d}x\mathrm{d}z}, \qquad \tilde{z}_i^n = \frac{\int_{\mathrm{Lag}_{\boldsymbol{Y}_i^n}(\psi)} z \, \mathrm{d}x\mathrm{d}z}{\int_{\mathrm{Lag}_{\boldsymbol{Y}_i^n}(\psi)} \mathrm{d}x\mathrm{d}z} \tag{5.8}$$

Before the next iteration of the time-step the points X_i^{n+1}, Z_i^{n+1} are mapped back to the fundamental domain.

5.3.2 Heun's Method

For comparison and to test convergence the time-stepping was also implemented using Heun's method [16].

$$\begin{aligned} t^{n+1} &= t^n + h, \quad \hat{Z}_i^{n+1} = Z_i^n + \frac{hCg}{f\theta_0}\left(X_i^n - \tilde{x}_i^n\right), \quad \hat{X}_i^{n+1} = X_i^n + \frac{hCg}{f\theta_0}\left(\tilde{z}_i^n - H/2\right) \\ Z_i^{n+1} &= Z_i^n + \frac{h}{2}\left(\frac{Cg}{f\theta_0}\left(X_i^n - \tilde{x}_i^n\right) + \frac{Cg}{f\theta_0}\left(\hat{X}_i^{n+1} - \hat{x}_i^{n+1}\right)\right) \\ X_i^{n+1} &= X_i^n + \frac{h}{2}\left(\frac{Cg}{f\theta_0}\left(\tilde{z}_i^n - H/2\right) + \frac{Cg}{f\theta_0}\left(\hat{z}_i^{n+1} - H/2\right)\right) \end{aligned} \tag{5.9}$$

Where again, $\hat{x}_i^n$ and $\hat{z}_i^n$ represent the centroids of the Laguerre cells given using 5.8 and $\hat{X}_i^{n+1}, \hat{Z}_i^{n+1}$ with corresponding weights given by the optimal transport algorithm DA.

Comment: why not higher order time-step method? Limited by OT solver - 2nd order?

Comment: include map back to fundamental domain explanation and why this isn't done for centroids

A comparison of results using Heun's method and the forward-Euler scheme for timestepping is detailed in Chapter 6.

5.4 Visualising the Output

Given the Geostrophic points and the associated weights which solve the optimal transport problem a Laguerre diagram satisfying 4.2.1 can be constructed. In the Monge-Ampère library of DA [13, 15] there is a function to rasterize a Laguerre diagram to a pixelated image, with Laguerre cells coloured according to the value of a particular variable.

For example, in the images below the Laguerre cells are coloured according to the value of θ' given by, $\theta' = \frac{f^2\theta_0 Z}{g}$

Chapter 6

Numerical Simulations and Results

6.1 Validating Results

6.1.1 Evolution of Average Kinetic Energy

The kinetic energy over the domain Γ is defined by,

$$E_{kin} = \int_{\Gamma} \frac{1}{2} v_g^2 \, dxdz \tag{6.1}$$

Given the geostrophic transformation 5.2 this can be expressed as,

$$E_{kin} = \int_{\Gamma} \frac{f^2}{2} (X - x)^2 \, dxdz \tag{6.2}$$

The kinetic energy associated with a fluid particle is the similarly defined as the integrals 6.1 and 6.2 but over the Laguerre cell of the point and its associated weight given by the solution of the optimal transport problem. **Comment: sort out domain averaged, show that solutions converge**

6.2 Error Analysis of the numerical Solution

Comment: discuss enery as error measurment, log-log plots for euler and heun and way to reduce error

6.3 Computational Performance

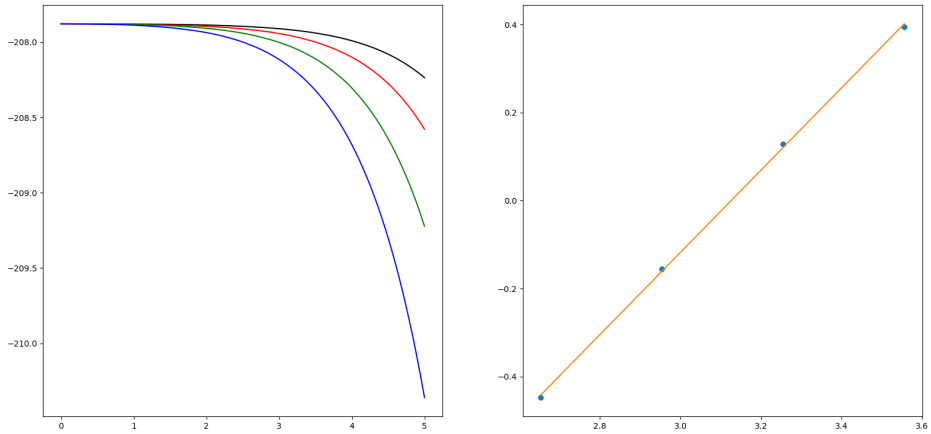

Figure 6.1

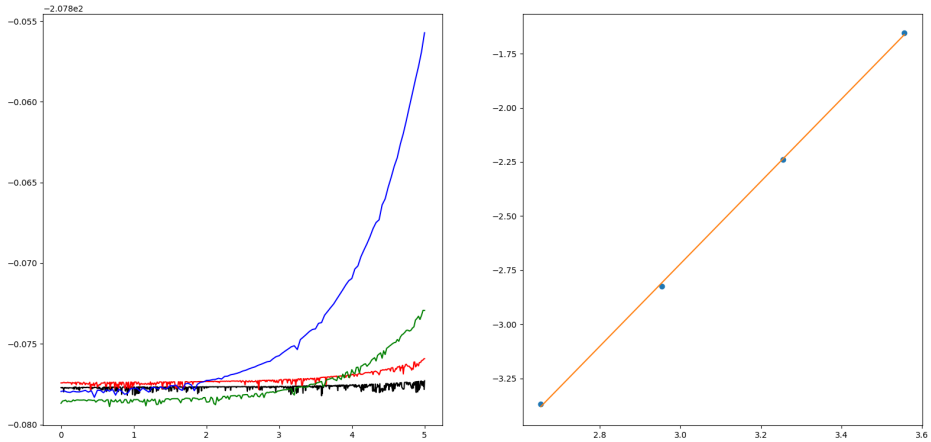

Figure 6.2

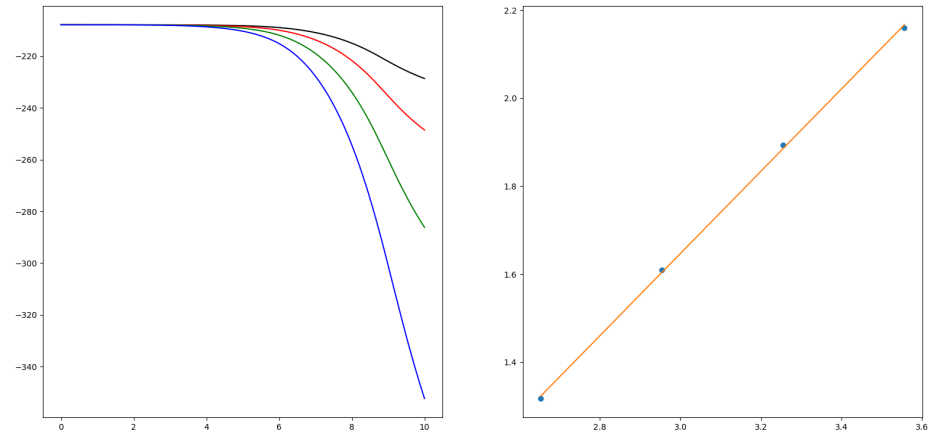

Figure 6.3

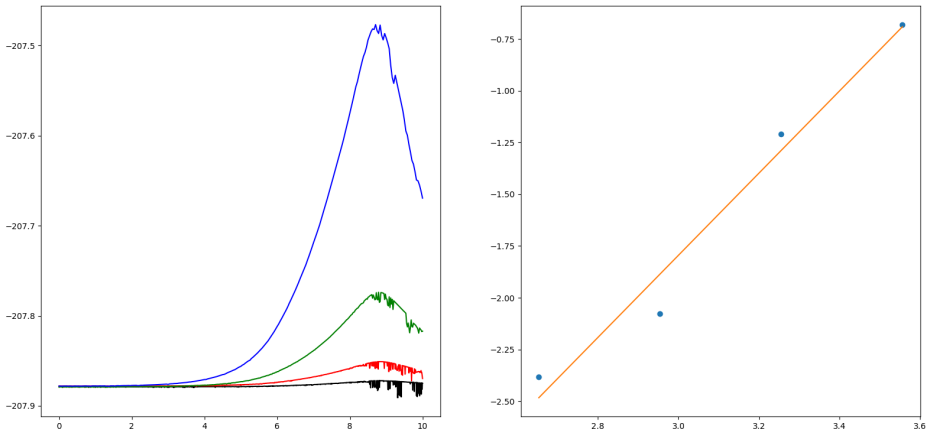

Figure 6.4

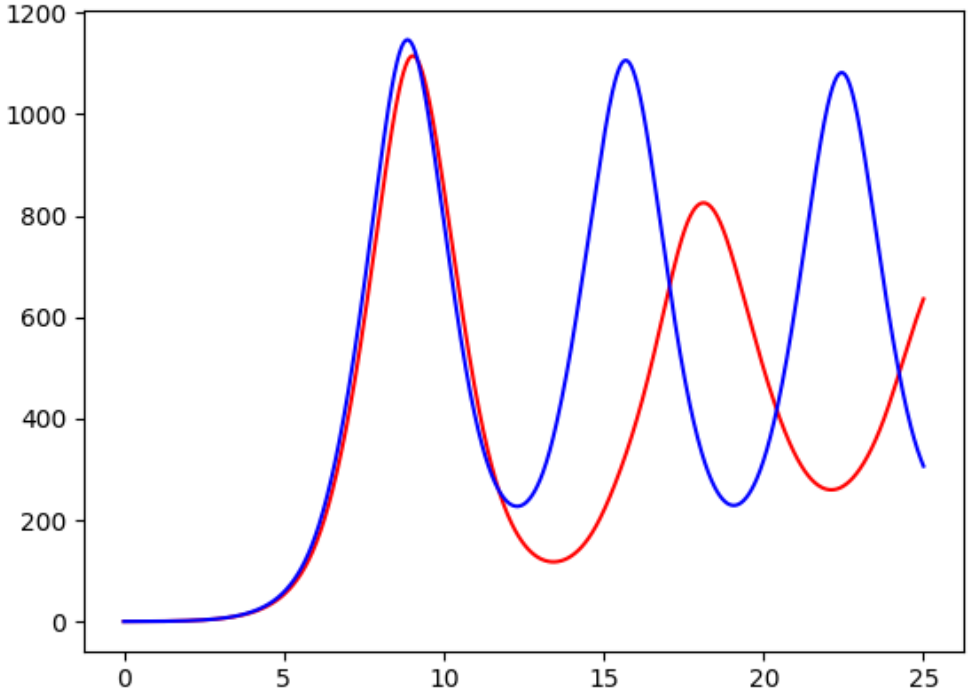

Figure 6.5

Chapter 7

Unsorted

7.1 Linear Stability Analysis

Starting from the Eady Model 2.11 restated below

$$\begin{aligned} -fv_g + \frac{\partial \varphi}{\partial x} &= 0, \\ \frac{Dv_g}{Dt} + fu - \frac{Cg}{\theta_0}(z - H/2) &= 0, \\ \frac{D\theta'}{Dt} - Cv_g &= 0, \\ \frac{\partial \varphi}{\partial z} - g\frac{\theta'}{\theta_0} &= 0, \\ \nabla \cdot \boldsymbol{u} &= 0. \end{aligned} \tag{7.1}$$

Linearise about a base state given by Hoskins [3],

$$\begin{aligned} \bar{\theta} &= \theta_0 \frac{N_0^2 \theta_0 z}{g} - Cy \\ \bar{\varphi} &= \theta_0 + \frac{N_0^2 z^2}{2} \\ \bar{v}_g &= 0 \\ \bar{U} &= \frac{Cg}{f\theta_0}(z - H/2) \\ \bar{W} &= 0 \end{aligned} \tag{7.2}$$

Introduce a perturbation and linearise about base state,
$u = \bar{U} + u'$, $w = w'$, $v_g = v_g'$, $\varphi = \bar{\varphi} + \varphi'$, $\theta' = \bar{\theta} + \theta''$
Introducing the stream function,

$$u' = \frac{\partial \psi}{\partial z}, \qquad w' = -\frac{\partial \psi}{\partial x} \tag{7.3}$$

Looking for normal modes solutions of the form,

$$q' = \hat{q}(z)\exp^{i(kx-\omega t)}$$

Equations 7.1 become,

$$-f\hat{v}_g + ik\hat{\varphi} = 0, \tag{7.4}$$

$$-i\omega\hat{v}_g + ik\bar{U}\hat{v}_g + f\frac{\mathrm{d}\hat{\psi}}{\mathrm{d}z} = 0, \tag{7.5}$$

$$-i\omega\hat{\theta} + ik\bar{U}\hat{\theta} - ik\frac{N_0^2\theta_0}{g}\hat{\psi} - C\hat{v}_g = 0, \tag{7.6}$$

$$\frac{\mathrm{d}\hat{\varphi}}{\mathrm{d}z} - g\frac{\hat{\theta}}{\theta_0} = 0, \tag{7.7}$$

First eliminating, φ, equations 7.4 and 7.7 give,

$$-f\frac{\mathrm{d}\hat{v}_g}{\mathrm{d}z} + ik\frac{\mathrm{d}\hat{\varphi}}{\mathrm{d}z} = 0, \qquad \frac{\mathrm{d}\hat{\varphi}}{\mathrm{d}z} - g\frac{\hat{\theta}}{\theta_0} = 0$$

so that,

$$\hat{\theta} = \frac{f\theta_0}{ikg}\frac{\mathrm{d}\hat{v}_g}{\mathrm{d}z} \tag{7.8}$$

Rearranging equation 7.6

$$i\left(k\bar{U} - \omega\right)\hat{\theta} - ik\frac{N_0^2\theta_0}{g}\hat{\psi} - C\hat{v}_g = 0 \tag{7.9}$$

Eliminating $\hat{\theta}$ using 7.8

$$\frac{f\theta_0}{kg}\left(k\bar{U} - \omega\right)\frac{\mathrm{d}\hat{v}_g}{\mathrm{d}z} - ik\frac{N_0^2\theta_0}{g}\hat{\psi} - C\hat{v}_g = 0$$

from equation 7.5 we have

$$i\left(k\bar{U} - \omega\right)\hat{v}_g - f\frac{\mathrm{d}\hat{\psi}}{\mathrm{d}z} = 0 \tag{7.10}$$

differentiating this expression we find

$$ik\frac{\mathrm{d}\bar{U}}{\mathrm{d}z}\hat{v}_g + i(k\bar{U} - \omega)\frac{\mathrm{d}\hat{v}_g}{\mathrm{d}z} + f\frac{\mathrm{d}^2\psi}{\mathrm{d}z^2} = 0$$

Substituting this expression with 7.10 into 7.9, noting that,

$$(k\bar{U} - \omega)\frac{\mathrm{d}\hat{v}_g}{\mathrm{d}z} = if\frac{\mathrm{d}^2\psi}{\mathrm{d}z^2} + \frac{fk}{i(k\bar{U} - \omega)}\frac{\mathrm{d}\bar{U}}{\mathrm{d}z}\frac{\mathrm{d}\hat{\psi}}{\mathrm{d}z}$$

$$\frac{f\theta_0}{kg}\left(if\frac{\mathrm{d}^2\psi}{\mathrm{d}z^2}+\frac{fk}{i(k\bar{U}-\omega)}\frac{\mathrm{d}\bar{U}}{\mathrm{d}z}\frac{\mathrm{d}\hat{\psi}}{\mathrm{d}z}\right)-\frac{ikN_0^2\theta_0\hat{\psi}}{g}+\frac{Cf}{i(k\bar{U}-\omega)}\frac{\mathrm{d}\psi}{\mathrm{d}z}=0$$

Rearranging gives,

$$-\frac{f^2\theta_0}{kg}(k\bar{U}-\omega)\frac{\mathrm{d}^2\psi}{\mathrm{d}z^2}+\left(Cf+\frac{f^2\theta_0}{g}\frac{\mathrm{d}\bar{U}}{\mathrm{d}z}\right)\frac{\mathrm{d}\hat{\psi}}{\mathrm{d}z}+\frac{kN_0^2\theta_0}{g}(k\bar{U}-\omega)\hat{\psi}=0$$

$$-f^2\theta_0(k\bar{U}-\omega)\frac{\mathrm{d}^2\psi}{\mathrm{d}z^2}+2Cfkg\frac{\mathrm{d}\hat{\psi}}{\mathrm{d}z}+k^2N_0^2\theta_0(k\bar{U}-\omega)\hat{\psi}=0$$

We reformulate this as a matrix eigenvalue problem for ω

$$-f^2\theta_0\bar{U}\frac{\mathrm{d}^2\psi}{\mathrm{d}z^2}+2Cfkg\frac{\mathrm{d}\hat{\psi}}{\mathrm{d}z}+k^2N_0^2\theta_0\bar{U}\hat{\psi}=\omega\left(k^2N_0^2\theta_0\hat{\psi}-f^2\theta_0\frac{\mathrm{d}^2\psi}{\mathrm{d}z^2}\right) \tag{7.11}$$

Introducing a second order finite difference scheme for ψ

$$\frac{\mathrm{d}^2\hat{\psi}}{\mathrm{d}z^2}=\frac{\psi_{i-1}-2\psi_i+\psi_{i+1}}{h^2}$$
$$\frac{\mathrm{d}\hat{\psi}}{\mathrm{d}z}=\frac{\psi_{i-1}-\psi_{i+1}}{2h}$$

Equation 7.11 becomes

$$\begin{aligned}-f^2\theta_0\bar{U}_i\left(\frac{\psi_{i-1}-2\psi_i+\psi_{i+1}}{h^2}\right)+2Cfkg\left(\frac{\psi_{i-1}-f\psi_{i+1}}{2h}\right)+k^3N_0^2\theta_0\bar{U}_i\psi_i=\\ \omega\left(k^2N_0^2\theta_0\psi_i-f^2\theta_0\left(\frac{\psi_{i-1}-2\psi_i+\psi_{i+1}}{h^2}\right)\right)\end{aligned} \tag{7.12}$$

Discretising the interval $[0,H]$ into N points with step size h we can recast this as an eigenvalue problem,

$$A\boldsymbol{\psi}=\omega B\boldsymbol{\psi}$$

to find eigenvalues ω with corresponding eigenvectors $\boldsymbol{\psi}=(\psi_1,...,\psi_{N-2})$. Since the boundary condition gives $\psi=0$ on $z=0,H$, $\psi_0=\psi_N=0$ so these are omitted from the $\hat{\phi}$ vector but considered in the finite difference schemes for ψ_1 and ψ_{N-1} The coefficients matrix A are given by

$$\begin{aligned}\psi_{i-1}:&\quad -\frac{-f^2\theta_0k\bar{U}_i}{h^2}-\frac{Cfkg}{h}\\ \psi_i:&\quad \frac{2f^2\theta_0k\bar{U}_i}{h^2}+k^3N_0^2\theta_0\bar{U}_i\\ \psi_{i+1}:&\quad \frac{-f^2\theta_0k\bar{U}_i}{h^2}+\frac{Cfkg}{h}\end{aligned} \tag{7.13}$$

$i : 1 \to N-2$ with $\psi_0 = \psi_N$. The coefficients of matrix B are given by,

$$\begin{aligned} \psi_{i-1} : &\quad -\frac{f^2\theta_0}{h^2} \\ \psi_i : &\quad k^2 N_0^2 \theta_0 + \frac{2f^2\theta_0}{h^2} \\ \psi_{i+1} : &\quad -\frac{f^2\theta_0}{h^2} \end{aligned}$$

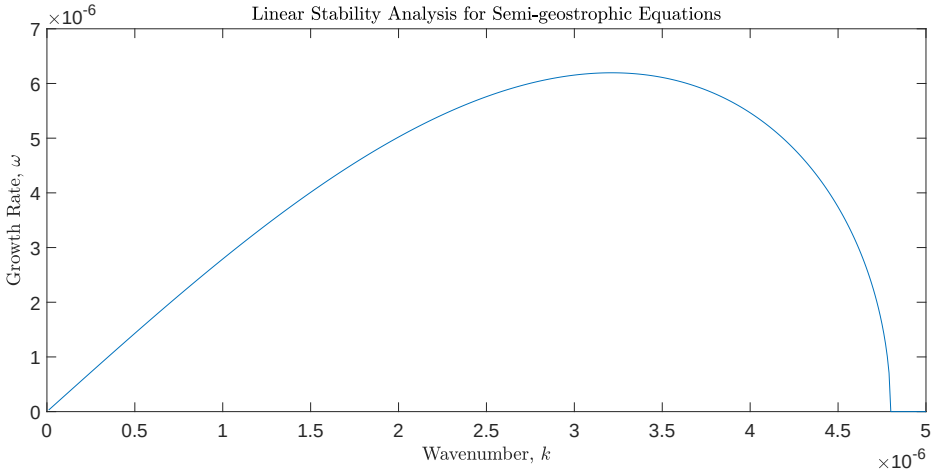

Figure 7.1: Plot showing growth rate, ω against wavenumber k for the Eady model of the semi-geostrophic equations

7.2 Calculation of Moments

For the implementation of the numerical algorithm for frontogenesis and subsequent analysis of its suitability, the moments of **Comment: word choice** the cells are required. Consider a point in geostrophic space $\boldsymbol{Y} = (X, Z)$ in the fundamental domain and corresponding weight ψ for which the Laguerre cell is $A = \mathrm{Lag}_{\boldsymbol{Y}}(\psi)$

O^{th} Moment

$$M_0 = \int_A dxdz \tag{7.14}$$

1^{st} Moment

$$M_{1x} = \int_A xdxdz, \qquad M_{1z} = \int_A zdxdz \tag{7.15}$$

2^{nd} Moment

$$M_{2x} = \int_A x^2 dxdz, \qquad M_{2z} = \int_A z^2 dxdz, \qquad M_{2xz} = \int_A xzdxdz \tag{7.16}$$

7.2.1 Considerations for Periodic Boundary Conditions

In implementing the moment calculations the periodicity of the domain needs to be carefully considered. For example, consider a point in geostrophic space (X, Z) in the fundamental domain and corresponding weight ψ it is possible that if X lies close to one of the limit points of the interval $[-L, L]$, that the centroid of the Laguerre cell associated with this point is exterior to the fundamental domain.

7.3 Ideas for extension

Chapter 8

Conclusion

Appendix A

First Appendix

Bibliography

[1] A. Eliassen. On the vertical circulation in the frontal zones. *Geofysiske Publikasjoner*, 4(4):147–160, 1962.

[2] Michael J P Cullen. *A Mathematical Theory of Large-scale Atmosphere/ocean Flow*. Imperial College Press, jan 2006.

[3] Brian J. Hoskins. The Geostrophic Momentum Approximation and the Semi-Geostrophic Equations. *Journal of the Atmospheric Sciences*, 32(2):233–242, 1975.

[4] B. J. Hoskins and F. P. Bretherton. Atmospheric Frontogenesis Models: Mathematical Formulation and Solution. *Journal of the Atmospheric Sciences*, 29(1):11–37, jan 1972.

[5] Hiroe Yamazaki, Jemma Shipton, Michael J.P. Cullen, Lawrence Mitchell, and Colin J. Cotter. Vertical slice modelling of nonlinear Eady waves using a compatible finite element method. *Journal of Computational Physics*, 343:130–149, aug 2017.

[6] Peter R. Bannon. Linear Baroclinic instability with the Geostrophic Momentum Approximation. *Journal of Atmospheric Sciences*, feb 1988.

[7] M. J.P. Cullen and I Roulstone. A geometric model of the non-linear equilibriation of two-dimensional Eady waves. *Journal of the Atmospheric Sciences*, 50:328–332, 1993.

[8] William Blumen. A Semigeostrophic Eady-Wave Frontal Model Incorporating Momentum Diffusion. Part I: Model and Solutions. *Journal of the Atmospheric Sciences*, 47(24):2890–2902, dec 1990.

[9] N. Nakamura. Nonlinear Equilibriation of Two-Dimensional Eady Waves: Simulations with Viscous Geostrophic Momentum Equations. *Journal of the Atmospheric Sciences*, 51:1023–1035, 1994.

[10] Yann Brenier and Mike Cullen. Rigorous derivation of the x-z semigeostrophic equations. *Communications in Mathematical Sciences*, 7(3):779–784, 2009.

[11] J.-D. Benamou and Y. Brenier. Weak existence for the semigeostrophic equations formulated as a coupled Monge-Ampère/transport problem. *SIAM J. Appl. Math.*, 58(5):1450–1461, oct 1998.

[12] Walter Rudin. *Real And Complex Analysis*. McGraw-Hill, 1986.

[13] Quentin Mérigot, Jocelyn Meyron, and Boris Thibert. An algorithm for optimal transport between a simplex soup and a point cloud. 2017.

[14] Jun Kitagawa, Quentin Mérigot, and Boris Thibert. Convergence of a Newton algorithm for semi-discrete optimal transport. 2016.

[15] Quentin Mérigot. PyMongeAmpere, python, 2017.

[16] David F. Griffiths and Desmond J. Higham. *Numerical Methods for Ordinary Differential Equations*, volume 79. 2010.